American Mineralogist, Volume 77, pages 784–794, 1992

Experimental investigation of melts from a carbonated phlogopite lherzolite: Implications for metasomatism in the continental lithospheric mantle

YVES THIBAULT,* ALAN D. EDGAR
Department of Geology, University of Western Ontario, London, Ontario N6A 5B7, Canada
FELICITY E. LLOYD
Department of Geoscience, University of Reading, Reading RG6 2AB, England

ABSTRACT

The composition of near-solidus melts formed from a model mantle of carbonated phlogopite lherzolite and phlogopite lherzolite was investigated at 3.0 GPa. At 1100 °C, the carbonated phlogopite lherzolite yielded 4 wt% of alkaline dolomitic melt coexisting with garnet-rich phlogopite lherzolite, whereas, at 1225 °C, the phlogopite lherzolite produced 7 wt% of hydrous potassic and calcic silicate melt in equilibrium with titaniferous phlogopite-bearing lherzolite.

The reactivity of these melts with peridotite was determined at 2.0 GPa and 1000 °C. Alkaline dolomitic melts can metasomatize harzburgite to olivine-rich phlogopite wehrlite, and infiltration in wehrlite may produce calcite-bearing phlogopite dunite. The interaction of harzburgite with the hydrous silicate melt results in enrichment in clinopyroxene and phlogopite.

A model of cyclic metasomatism active beneath a continental rift is proposed. A horizon of carbonated phlogopite lherzolite, originally formed at the base of the lithosphere by the release of dense alkaline fluids from a hot mantle plume, migrates upward by means of cycles of melting, migrating, solidifying, and reacting as rifting progresses. At a depth of 100 km, fractional melting of the carbonated phlogopite lherzolite horizon yields successively an alkaline dolomitic melt and a hydrous potassic and calcic silicate melt. The infiltration of these distinct melts into depleted lithospheric mantle at 65-km depth results in a decoupled metasomatic event. First, metasomatism by the dolomitic melt creates a trend from harzburgite to olivine-rich wehrlite. The subsequent infiltration of the silicate melt enriches the metasomatized rocks in clinopyroxene and phlogopite. The variety of rocks that result bears similarities with a suite of mantle xenoliths from the West Eifel volcanic field, Germany.

INTRODUCTION

Carbonatitic and hydrous mafic silicate liquids may segregate from their mantle sources and migrate by infiltration even at melt fractions of 1% or less (e.g., McKenzie, 1985; Hunter and McKenzie, 1989). Such small volumes of melts will probably experience thermal crisis (e.g., Spera, 1984) or be consumed in metasomatic reactions during migration into the overlying colder lithospheric mantle (McKenzie, 1989). These considerations emphasize the importance of (1) characterizing the composition of volatile-bearing low-degree partial melts formed from hydrated and carbonated mantle sources, and (2) investigating the reactivity of these liquids with depleted peridotitic material.

This paper reports the results of an investigation of near-solidus melt fractions formed from phlogopite-bearing mantle compositions. Two types of experiments were performed: (1) partial melting of a model mantle of carbonated phlogopite lherzolite and phlogopite lherzolite; and (2) melt-peridotite interaction experiments on harzburgitic and wehrlitic materials. The results complement previous investigations that have dealt with the nature (e.g., Olafsson and Eggler, 1983; Wallace and Green, 1988) and reactivity (e.g., Meen, 1987; Green and Wallace, 1988; Meen et al., 1989) of melts formed from amphibole-bearing carbonated peridotitic sources.

EXPERIMENTAL AND ANALYTICAL TECHNIQUES

Starting materials

The model mantle compositions (Table 1) were prepared using mineral separates, Spec Pure $CaCO_3$, and Fisher Certified Na_2CO_3. Fresh olivine, orthopyroxene, clinopyroxene, and spinel grains were separated from a lherzolite xenolith (E48Y; Lloyd et al., 1991) from the West Eifel volcanic field, Germany. Phlogopite is from a single xenocryst also sampled from the West Eifel volcanic field. The dried materials were mixed and ground

* Present address: Department of Geology, Arizona State University, Tempe, Arizona 85287, U.S.A.

0003–004X/92/0708–0784$02.00

TABLE 1. Compositions of synthesized starting materials

	CPL	CPL[c]	PLZ	PLZ[c]	HAR	WHR	Carmet	Silmet
				Chemical composition (wt%)				
SiO_2	45.07	44.93	47.04	46.94	48.31	42.33	1.16	45.81
TiO_2	0.29	0.29	0.30	0.30	0.01	0.03	0.28	1.67
Al_2O_3	4.05	4.06	4.23	4.24	1.52	2.36	0.21	12.14
Cr_2O_3	0.69	0.69	0.72	0.72	0.15	0.65	0.00	0.00
FeO_{tot}	6.44	6.51	6.72	6.79	7.43	7.62	4.25	6.51
MnO	0.11	0.11	0.12	0.12	0.13	0.12	0.15	0.00
MgO	33.92	34.23	35.40	35.76	42.00	40.96	15.16	11.75
NiO	0.11	0.11	0.11	0.11	0.15	0.22	0.00	0.00
CaO	6.09	5.80	4.32	3.98	0.28	5.50	28.57	11.29
Na_2O	0.60	0.60	0.20	0.19	0.02	0.21	2.94	2.27
K_2O	0.58	0.59	0.61	0.62	0.00	0.00	3.99	6.20
H_2O	0.22	0.22	0.23	0.23	0.00	0.00	1.61	2.36
CO_2	1.83	1.86	0.00	0.00	0.00	0.00	41.68	0.00
Total	100.00	100.00	100.00	100.00	100.00	100.00	100.00	100.00
X_{MgFe}	0.90	0.90	0.90	0.90	0.91	0.91	0.86	0.76

Note: CPL[c] and PLZ[c] are corrected bulk compositions calculated by subtraction of 10% of the total amount of clinopyroxene. H_2O and CO_2 are calculated assuming perfect stoichiometry in the carbonated and hydrous minerals used in the synthesis. X_{MgFe} represents $Mg/(Mg + Fe_{tot})$.

together under acetone to a grain size of approximately 10 μm.

The two model mantle sources have mineral contents representative of carbonated phlogopite lherzolite (CPL; Table 1) and phlogopite lherzolite (PLZ; Table 1). The proportion of olivine incorporated in the mixtures was kept low ($\approx$40%) in order to enhance the proportion of the minor phases, thereby facilitating their identification and analysis (cf. Green and Ringwood, 1970). The relative abundance of phlogopite and carbonates in the source, which is essentially related to the amount of CO_2, H_2O, and alkalis, has a significant effect on near-solidus melting relationships (e.g., Holloway and Eggler, 1976). However, no unequivocal samples of natural metasomatized carbonate-bearing peridotite, upon which a starting composition may be chosen, have been reported. This is probably because of the very rapid decomposition of carbonates in mantle xenoliths during ascent in their host magma (e.g., Canil, 1990). Therefore, the CO_2, H_2O, and total alkali contents of the CPL source were kept close to those of the starting material used by Wallace and Green (1988), which allowed a consistent comparison with recent experimental results on carbonated amphibole-bearing peridotite. However, the K_2O-Na_2O value is significantly higher in CPL, reflecting a characteristic of many xenoliths of phlogopite-bearing garnet lherzolite (e.g., Erlank et al., 1987, their Table IVb).

One model mantle protolith for the experiments on melt-peridotite interaction was harzburgitic (HAR; Table 1), a composition abundant and widespread in the mantle xenolith population (e.g., Harte and Hawkesworth, 1989). A spinel wehrlite protolith (WHR; Table 1) was also prepared.

Hydrous silicate melt compositions were synthesized in a two-stage process. First, mixtures of the required amounts of dried SiO_2, TiO_2, Al_2O_3, MgO, $CaCO_3$, Na_2CO_3, and K_2CO_3 were melted in air at 1350 °C for 30 min to remove CO_2 and quenched to a glass. Then, mixtures of the appropriate amounts of synthesized glass, natural fayalite (source of FeO), and brucite (source of H_2O) were sealed in Pt capsules and melted in a piston-cylinder apparatus at 1.2 GPa and 1350 °C for 5 min. The products were hydrous glasses whose compositions were checked by microprobe analyses. Carbonate melt compositions were synthesized as simple mixtures of dried $CaCO_3$, Na_2CO_3 and K_2CO_3 and natural dolomite and brucite.

Experimental procedures

The pressure-temperature conditions were achieved in a piston-cylinder apparatus and furnace assemblies with a diameter of 1.27 cm (Boyd and England, 1960), using the so-called piston-out technique after achieving the desired temperature of the experiment. The pressure-transmitting medium consisted of a talc-Pyrex sleeve. A graphite furnace was used, and the temperature was monitored using a Pt-$Pt_{90}Rh_{10}$ thermocouple. No frictional correction was applied to pressure nor a pressure correction to the emf of the thermocouple. In principle, pressure and temperature could be controlled to within $\pm$0.05 GPa and $\pm$5 °C of the stated values. The starting material was sealed into $Ag_{50}Pd_{50}$ capsules. Normally, experimental times ranged from 28 to 8 h.

An estimation of the f_{O_2} was made in experiments where olivine, orthopyroxene, and spinel coexist in the product, using the semiempirical O geobarometer proposed by Ballhaus et al. (1991). The calculation of the Fe^{3+} content of spinel assumed perfect R_3O_4 stoichiometry (e.g., Mattioli et al., 1989; Ballhaus et al., 1991). The log f_{O_2} obtained is within 0.5 log units of the fayalite + magnetite + quartz (FMQ) O buffer.

The liquid compositions at low degrees of partial melting of the two model mantle sources, CPL and PLZ, were determined using a sandwich technique, in which 10–18 wt% of an estimated melt composition is added between two layers of the peridotite source. This technique ensures that large areas of melt, whose composition is not affected by quench overgrowths on primary residual crys-

TABLE 2. Experimental results

Partial melting experiments

Starting material	T (°C)	t (h)	Stable phases
CPL	900	28	ol, opx, cpx, phl, mag
CPL	925	28	ol, opx, cpx, phl, mag
CPL	975	20	ol, opx, cpx, phl, mag
CPL	1000	28	ol, opx, cpx, phl, mag
CPL	950–>1025	21–>5	ol, opx, cpx, phl, mag, dol
CPL	950–>1050	20–>5	ol, opx, cpx, phl, dol
CPL	950–>1075	21–>4.5	ol, opx, cpx, phl, gar, liq
CPL	950–>1100	20–>5	ol, opx, cpx, phl, gar, liq
CPL	950–>1125	20–>4	ol, opx, cpx, phl, gar, liq
CPL	950–>1150	20–>4	ol, opx, cpx, phl, gar, liq
CPL (SDW1)	1100	9.5	ol, opx, cpx, gar, liq
CPL (SDW2)	1100	9.5	ol, opx, cpx, phl, gar, liq
CPL (SDW3A)	1100	9.5	ol, opx, cpx, phl, gar, liq
CPL (SDW3B)	1100	1	ol, opx, cpx, phl, gar, liq
PLZ	1125	28	ol, opx, cpx, phl, gar
PLZ	1150	28	ol, opx, cpx, phl, gar
PLZ	1175	20	ol, opx, cpx, phl, gar, liq
PLZ	1200	20	ol, opx, cpx, phl, gar, liq
PLZ	1225	19	ol, opx, cpx, phl, gar, liq
PLZ	1235	20	ol, opx, cpx, phl, gar, liq
PLZ	1250	10	ol, opx, cpx, phl, gar, liq
PLZ (SDW1)	1225	8	ol, opx, cpx, phl, gar, liq
PLZ (SDW2A)	1225	8	ol, opx, cpx, phl, gar, liq
PLZ (SDW2B)	1225	1	ol, opx, cpx, phl, gar, liq

Melt-peridotite interaction experiments

Starting material	T (°C)	t (h)	Weight ratio*	Stable phases
HAR	1000	28	0:100	ol, opx
WHR	1000	28	0:100	ol, opx, sp
Carmet-HAR	1000	20	90:10	ol, opx, cpx, phl, v
Carmet-WHR	1000	20	90:10	ol, cpx, sp, cc, phl, v
Silmet-HAR	1200–>1000	1–>'22	75:25	ol, opx, cpx, phl

Note: The notations m–>n and x–>$^z y$ for temperature and times, respectively, mean that the experiment was conducted x h at m °C, then brought to n °C gradually in z h, and then maintained y h at n °C. Abbreviations: ol = olivine; opx = orthopyroxene; cpx = clinopyroxene; phl = phlogopite; gar = garnet; mag = magnesite; dol = dolomite; liq = liquid; sp = spinel; cc = calcite; v = vapor phase. Stable phases do not include relict phases observed in trace amounts. (SDWX) refers to the Xth iteration for the sandwich experiment.

* Expresses the melt/peridotite ratio of the mixture in weight percent.

tals, are available for defocused electron beam microprobe analyses (Fujii and Scarfe, 1985). An iterative method was adopted in which the composition of the melt, determined after an initial sandwich experiment, is used as a guide for the synthesis of the melt layer of the subsequent sandwich experiment (cf. Wallace and Green, 1988). The composition of the quench liquid is considered to be near that of the melt ideally in equilibrium with the residual mantle source when: (1) the mineral assemblage in the sandwich experiment is the same as that of the nonsandwich experiment at the same pressure-temperature conditions, and (2) the composition of the corresponding residual minerals in the two types of experiments are very close. The iteration experiments were done with durations of 9.5 and 8 h. When the two criteria described above were fulfilled, an additional sandwich experiment of 1 h was performed to minimize Fe loss effect on the determined melt composition (cf. Mengel and Green, 1989).

Attainment of equilibrium

In the products of the melting experiments, most crystalline phases are compositionally uniform. Only large clinopyroxene grains (>10 μm) have slight zonation with relict composition in the cores. The rims of these larger grains have a composition similar to very small homogeneous clinopyroxene crystals ($\leq$2 μm) in close contact with the melt, suggesting that the clinopyroxene rims have likely reacted fully with the liquid (cf. Fujii and Scarfe, 1985). Moreover, the unreacted central portion of the clinopyroxene crystals is quite small (<10% of the grain). Assuming that 10% of the total amount of clinopyroxene (estimated maximum amount of relict cores) was not part of the system, new bulk compositions of the CPL and PLZ model sources could be calculated (Table 1). Because these corrected bulk compositions are very close to the original ones, we considered that adequate equilibrium conditions have been attained. When needed in melting-reaction calculation, the original and corrected bulk com-

TABLE 3. Comparison of representative compositions of phases obtained in nonsandwich and sandwich melting experiments

Source	CPL (1100 °C)						PLZ (1225 °C)					
Phase	cpx		phl		gar		cpx		phl		gar	
Type	N-SDW	SDW3B	N-SDW	SDW3B	N-SDW	SDW3B	N-SDW	SDW2B	N-SDW	SDW2B	N-SDW	SDW2B
	Compositions in wt%											
SiO_2	52.91	52.95	37.45	38.58	41.38	41.44	52.26	52.63	37.81	38.76	42.30	42.12
TiO_2	0.09	0.09	5.52	5.45	1.72	1.41	0.14	0.15	7.04	6.56	0.69	0.56
Al_2O_3	3.74	3.50	17.71	17.37	21.41	20.96	4.48	4.20	16.12	16.93	20.44	21.51
Cr_2O_3	0.46	0.51	0.34	0.61	1.32	1.39	0.63	0.98	1.54	0.39	3.12	2.49
FeO_{tot}	2.97	2.82	4.54	4.82	7.20	7.55	2.92	2.94	4.04	4.22	5.16	5.93
MnO	0.08	0.16	0.04	0.10	0.33	0.34	0.11	0.06	0.06	0.05	0.25	0.26
MgO	16.72	16.38	20.02	19.74	19.27	19.19	17.21	17.20	19.03	18.87	20.81	19.97
CaO	22.26	22.33	0.54	0.35	7.60	7.56	20.90	20.89	0.21	0.04	7.13	6.96
Na_2O	0.85	0.81	0.10	0.13	0.00	0.00	0.73	0.83	0.03	0.10	0.00	0.00
K_2O	0.00	0.00	9.43	9.82	0.00	0.00	0.00	0.03	10.43	10.44	0.00	0.00
Total	100.08	99.55	95.69	96.97	100.23	99.84	99.38	99.91	96.31	96.36	99.90	99.80
	Cations per O atoms*											
	(6)	(6)	(22)	(22)	(24)	(24)	(6)	(6)	(22)	(22)	(24)	(24)
Si	1.9210	1.9322	5.3058	5.4027	5.9137	5.9548	1.9040	1.9089	5.3577	5.4563	6.0191	6.0003
$^{[4]}Al$	0.0790	0.0678	2.6942	2.5973	0.0863	0.0452	0.0960	0.0911	2.6423	2.5437	0.0000	0.0000
$^{[6]}Al$	0.0811	0.0828	0.2639	0.2705	3.5208	3.5057	0.0964	0.0885	0.0512	0.2660	3.4289	3.6125
Ti	0.0025	0.0023	0.5882	0.5740	0.1849	0.1524	0.0038	0.0041	0.7503	0.6945	0.0738	0.0600
Cr	0.0132	0.0146	0.0381	0.0675	0.1491	0.1579	0.0181	0.0281	0.1728	0.0434	0.3510	0.2804
Fe	0.0902	0.0859	0.5379	0.5645	0.8605	0.9073	0.0890	0.0892	0.4785	0.4968	0.6141	0.7065
Mn	0.0025	0.0049	0.0048	0.0119	0.0399	0.0414	0.0034	0.0018	0.0075	0.0060	0.0301	0.0314
Mg	0.9047	0.8906	4.2271	4.1198	4.1042	4.1097	0.9345	0.9297	4.0190	3.9588	4.4131	4.2398
Ca	0.8660	0.8732	0.0820	0.0525	1.1638	1.1640	0.8159	0.8119	0.0323	0.0060	1.0871	1.0624
Na	0.0598	0.0571	0.0275	0.0353	0.0000	0.0000	0.0516	0.0584	0.0082	0.0273	0.0000	0.0000
K	0.0000	0.0000	1.7045	1.7545	0.0000	0.0000	0.0000	0.0014	1.8861	1.8750	0.0000	0.0000
Total	4.0200	4.0114	15.4740	15.4505	16.0232	16.0384	4.0127	4.0130	15.4059	15.3738	16.0172	15.9933
$X_{MgFe_{tot}}$	0.91	0.91	0.89	0.88	0.83	0.82	0.91	0.91	0.89	0.89	0.88	0.86

Note: Abbreviations as in Table 2; N-SDW represents nonsandwich experiment; SDW*X* refers to the *X*th iteration for the sandwich experiment (see Table 2).

* Number of O atoms in parentheses at head of columns.

positions were both used in order to semiquantify the effects of this potential problem. In the products of the interaction experiments no compositional zonation were observed.

Analytical methods

Longitudinal sections of the experimental charges were mounted and polished for microprobe analysis. To avoid possible dissolution of alkali-bearing carbonates, H_2O was not used in the preparation of polished sections for the products of the experiments on the CPL composition (cf. Wallace and Green, 1988). Wavelength dispersive analyses of all phases were conducted on a JEOL JXA-8600 electron microprobe. All elements were analyzed at 15-kV accelerating voltage with a 10-nA beam current. Matrix corrections were made using the Tracor Northern ZAF program.

Results for CPL mantle source at 3.0 GPa

Phase relationships

Temperatures for the melting experiments on the CPL mantle composition at 3.0 GPa ranged from 900 to 1150 °C. Olivine, orthopyroxene, clinopyroxene, and phlogopite were stable at those temperatures (Table 2). Garnet was abundant in experiments from 1075 to 1150 °C but could not be observed at subsolidus conditions (Table 2), probably because of lack of time for nucleation at such low temperatures. Well-crystallized carbonates were stable up to 1050 °C. At higher temperatures only small interstitial acicular grains of carbonate were observed, probably quenched from a CO_2-rich melt. The solidus for the CPL composition at 3.0 GPa occurred, therefore, near 1060 °C. This temperature significantly exceeds the one obtained by Wallace and Green (1988) for the solidus of their carbonated peridotite (<1000 °C) at pressures greater than amphibole breakdown (≈carbonated phlogopite lherzolite). This is probably because of the fact that CPL melts under fluid-absent conditions, in contrast to the source used by Wallace and Green (1988), which coexists with free H_2O released by amphibole breakdown at high pressure.

Chemical composition of minerals

Olivine and orthopyroxene have relatively constant compositions throughout the investigated temperature interval. Clinopyroxene is an aluminian chromian diopside (Table 3). At suprasolidus conditions, the clinopyroxene grains show lower Na content ($Na_2O \approx 0.8$ wt%) than the subsolidus ones ($Na_2O \approx 1.5$ wt%).

Phlogopite has high TiO_2 contents (Table 3). As melting proceeds, the ratio of Ti/K in phlogopite increases

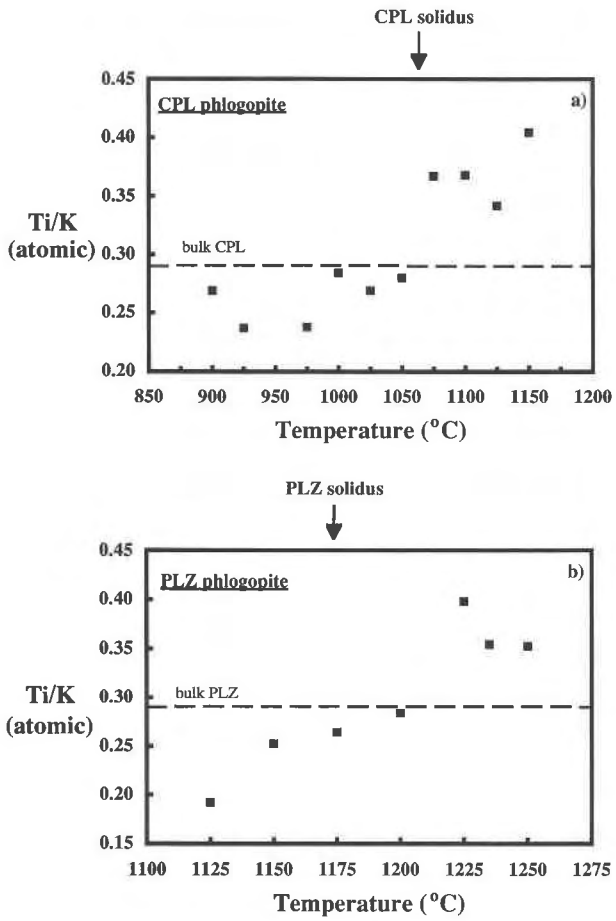

Fig. 1. Variation of the Ti/K atomic ratio of phlogopite against temperature in the melting experiments on (**a**) the CPL and (**b**) the PLZ model mantle sources. Because the amount of K is relatively constant in phlogopite, Ti-K variation represents essentially the change in the abundance of Ti. The dashed lines represent the Ti/K ratios calculated for the model sources bulk compositions. As long as phlogopite represents the only K-bearing phase, these bulk Ti/K ratios should define the maximum Ti content that phlogopite can contain.

markedly to values in excess of 0.29, calculated for the bulk CPL mantle composition (Fig. 1a). A high ratio of Ti/K for suprasolidus phlogopite suggests that the coexisting melt contains a significant amount of K with a low Ti/K ratio.

As the solidus is crossed, garnet becomes abundant. Its pyrope component ranges from 64.8 to 67.3 mol%. As shown in Figure 2, garnet from the melting experiments on the CPL composition is rich in TiO_2 (≈2 wt%) and relatively poor in Cr_2O_3 (<2 wt%).

The stable carbonate phase is magnesite ($MgCO_3$ ≈ 86 mol%) from 900 to 1025 °C. It is then replaced by dolomite ($MgCO_3$ ≈ 48 mol%) up to 1050 °C (cf. Brey et al., 1983; Olafsson and Eggler, 1983; Falloon and Green, 1989).

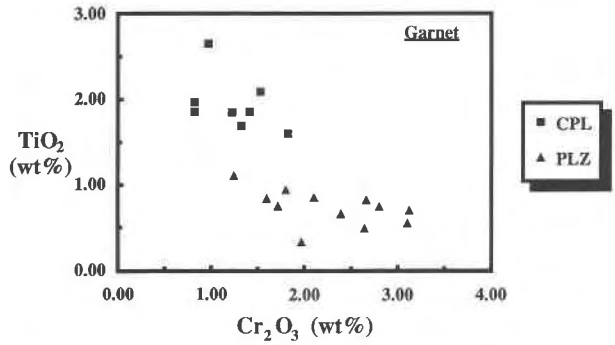

Fig. 2. Diagram of TiO_2 (wt%) against Cr_2O_3 (wt%) in garnet observed in the melting experiments on the CPL and the PLZ model mantle sources.

Melt composition at 3.0 GPa and 1100 °C

Sandwich experiments using the iterative method described earlier were performed at 1100 °C and 3.0 GPa. The synthesized melt composition for the initial sandwich experiment was a sodic dolomitic melt (Table 4, analysis A). Three iterative steps were needed to obtain residual mineral compositions very close to those in the nonsandwich experiment at 1100 °C (Table 3). The composition of the melt (Table 4, analysis B) was estimated by defocused electron beam microprobe analyses of large melt pools consisting of aggregates of acicular quenched carbonate grains. The melt has a strong dolomitic affinity, very low contents of SiO_2, Al_2O_3, and TiO_2 and a significant amount of alkalis. Because K was supplied by the partial breakdown of phlogopite, and no other hydrous minerals were observed, the synthesized melt composition in each iteration step contained H_2O in an amount defining a H_2O/K_2O weight ratio near that of hydrous phlogopite ($H_2O/K_2O \approx 0.38$). Finally, the $X_{MgFe_{tot}}$ value of the melt is high. Although this can be partially explained by Fe loss to the $Ag_{50}Pd_{50}$ capsule, Green and Wallace (1988) have also reported that Mg-Fe fractionation between solid silicates and alkaline dolomitic carbonatite melt is significantly smaller than for silicate melts.

The composition of all the residual minerals and of the liquid were used together with the bulk CPL composition (either original or corrected) in a least-squares mass-balance calculation to estimate the weight proportion of the phases stable at 1100 °C. The calculation suggests that the CPL model source yields 4 wt% of alkaline dolomitic melt, and, as observed in the experimental product, the proportion of garnet is quite high (10 wt%). The reactions controlling the phlogopite-present melting interval of the CPL model source at 3.0 GPa can be qualitatively defined as

$$\text{dolomite}_{solid} + \text{phlogopite}_{ss} + \text{clinopyroxene}_{ss} \rightarrow \text{dolomite}_{melt} + (K,Na,OH)_{melt} + \text{olivine}_{ss} + \text{pyrope}_{ss}\ (\text{rich in Ti}) + \text{residual phlogopite}_{ss}\ (\text{rich in Ti}) + \text{residual clinopyroxene}_{ss} \quad (1)$$

TABLE 4. Average melt compositions

Oxide	A	B	C	D	CIPW	Norm (D)
SiO_2		2.57	44.83	47.96	Or	7.25
TiO_2		0.72	2.12	1.68	An	9.53
Al_2O_3		0.38	15.48	10.97	Lc	19.81
Cr_2O_3		0.00		0.29	Ne	4.86
FeO_{tot}	5.61	4.54	7.36	5.66	Di	38.83
MnO	0.13	0.16	0.10	0.15	Ol	14.60
MgO	15.40	15.12	11.46	13.21	Mt	1.59
CaO	24.95	21.60	6.06	11.59	Il	3.25
Na_2O	8.19	4.93	1.13	1.04		
K_2O		7.01	8.30	5.40		
H_2O		2.66	3.16	2.05		
CO_2	45.72	40.31				
Total	100.00	100.00	100.00	100.00		
$X_{Mg/Fe_{tot}}$	0.83	0.86	0.74	0.81		

Note: A and C are synthesized melt compositions used in the initial sandwich experiments on the CPL (A) and PLZ (C) sources. B and D are final compositions of melts obtained by sandwich experiments on the CPL (B) and PLZ (D) sources. D was normalized to 100 wt% (real total anhydrous: 96.01 wt%). Its norm was obtained with a calculated ratio of Fe_2O_3/FeO (Kress and Carmichael, 1988) for f_{O_2} of the QFM buffer (Myers and Eugster, 1983) at 1225 °C. H_2O was calculated for a H_2O/K_2O weight ratio of 0.38. CO_2 was calculated by the stoichiometry of the carbonates in A and the deficiency in the total of oxides in B. Na_2O in D is calculated using the phase proportions obtained by least-squares mass balance.

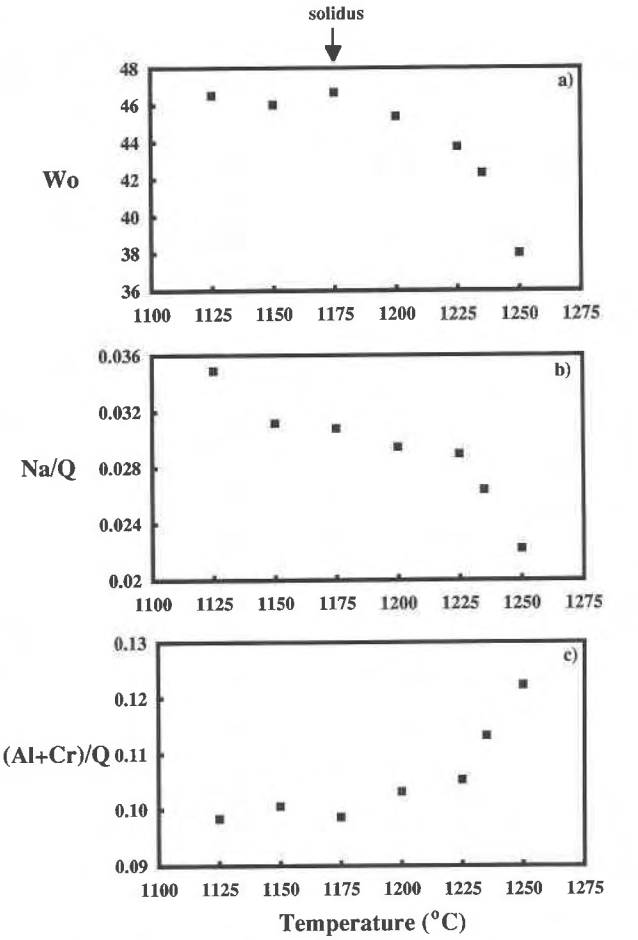

Fig. 3. Variation of (**a**) Wo = 100x[Ca/(Ca + Mg + Fe + Mn)], (**b**) Na/Q = Na/(Ca + Mg + Fe + Mn), and (**c**) (Al + Cr)/Q = (Al + Cr)/(Ca + Mg + Fe + Mn) in clinopyroxene against temperature for the melting experiments on the PLZ model mantle source. All ratios are atomic.

where ss means solid solution. In addition to the complete melting of dolomite at the solidus, Reaction 1 describes the partial breakdown of phlogopite and clinopyroxene (jadeite component) to yield K, Na, and OH to the melt (cf. Wallace and Green, 1988). SiO_2, Al_2O_3, MgO, FeO, and TiO_2, also released from the breakdown of phlogopite and clinopyroxene, are combined to form olivine and pyrope. This explains the high abundance of garnet rich in TiO_2 (Fig. 2).

Implications for the subsequent experiments

If carbonated phlogopite lherzolite composition comparable to CPL exists in the upper mantle, alkaline dolomitic melt may be formed and easily migrate upward by infiltration caused by its low viscosity (Hunter and McKenzie, 1989), leaving behind a residual CO_2-free garnet-bearing phlogopite lherzolite. The experiments on the PLZ composition were performed to investigate the composition of the near-solidus melt formed from such a residual mantle source.

Results for PLZ mantle source at 3.0 GPa

Phase relationships

Olivine, orthopyroxene, clinopyroxene, garnet, and phlogopite were stable throughout the investigated temperature interval ranging from 1125 to 1250 °C (Table 2). On the basis of the appearance of interstitial glass and a significant decrease in the abundance of phlogopite, the solidus was estimated at 1175 °C (Table 2), a temperature in accordance with the solidus temperature obtained by Wendlandt and Eggler (1980, their Fig. 1) on a comparable phlogopite lherzolite.

Chemical composition of minerals

Olivine and orthopyroxene have relatively constant compositions. With increasing temperature, clinopyroxene shows a systematic decrease in the proportion of wollastonite component (Fig. 3a). Also observed in clinopyroxene, from the solidus temperature to 1250 °C, are a decrease in Na (Fig. 3b) and an increase in (Al_{tot} + Cr) (Fig. 3c), relative to the quadrilateral components (Ca + Mg + Fe + Mn).

Phlogopite is rich in TiO_2 with the ratio of Ti/K increasing steadily with temperature (Fig. 1b). At suprasolidus conditions, Ti/K ratios in excess of 0.29 calculated for the bulk PLZ composition (Fig. 1b) suggest that the melt is enriched in K with Ti partitioned preferentially in the coexisting phlogopite.

The pyrope component of garnet ranges from 68.9 to 72.5 mol%. Compared to garnet observed in the melting

of the CPL composition, PLZ garnet is poorer in TiO_2 and generally richer in Cr_2O_3 (Fig. 2).

Melt composition at 3.0 GPa and 1225 °C

Sandwich experiments were performed at 1225 °C. The composition of the synthesized glass used in the initial sandwich experiment (Table 4, analysis C) was based on electron microprobe analyses of small melt pools from the nonsandwich experiment at 1225 °C. The amount of H_2O added to the synthesized glass was defined using a H_2O/K_2O weight ratio of 0.38, typical of hydrous phlogopite.

Two iterative steps were needed to obtain a good approximation of the equilibrium partial melt of the PLZ source at 1225 °C. The melt layer showed a homogeneous texture consisting of glass and small acicular quench grains of clinopyroxene. Analyses of the quench liquid (glass + quench clinopyroxene) were obtained with the microprobe using a defocused electron beam with a diameter of 10–30 μm. The average composition is presented in Table 4 (analysis D). The melt is strongly potassic ($K_2O \approx 5$ wt%) and silica undersaturated. The major normative components are diopside, leucite, olivine, and anorthite, reflecting the major role of clinopyroxene and phlogopite in the melting reaction. The $X_{Mg/Fe_{tot}}$ value of 0.81 is significantly lower than for the melt obtained from the CPL source. The composition found by Mengel and Green (1989) for a melt coexisting with phlogopite-bearing peridotitic assemblage at 2.8 GPa and 1195 °C using comparable sandwich techniques bears similarities to the melt formed from PLZ at 1225 °C but is clearly less potassic ($K_2O \approx 1.6$ wt%). This difference probably results from the fact that, in contrast to the melting conditions of this study, the H_2O/alkali ratio in Mengel and Green's source is such that there is an excess of H_2O relative to the amount needed to form phlogopite when amphibole breaks down at high pressure.

The weight proportions of the phases stable at 1125 and 1225 °C were calculated by least-squares mass balance. Based on the results, a generalized melting reaction describing the phlogopite-present melting interval of the PLZ model source at 3.0 GPa would be

$$\begin{aligned} &3.8(4.3)\ \text{phlogopite} + 3.7(3.5)\ \text{clinopyroxene} \\ &+ 0.8(0.8)\ \text{garnet} \\ &\quad \rightarrow 1.1(1.2)\ \text{olivine} + 0.0(0.4)\ \text{orthopyroxene} \\ &\qquad + 7.1(7.0)\ \text{liquid} \end{aligned} \tag{2}$$

where the values in parentheses are calculated using the corrected bulk composition of PLZ (Table 1, PLZ^c). The degree of partial melting at 1225 °C is, therefore, estimated at 7 wt%. In contrast to the relations observed for the CPL composition (Reaction 1), garnet is a reactant of melting Reaction 2 due to the high compatibility of Al_2O_3, SiO_2, and TiO_2 in the silicate melt. This explains the lower TiO_2 and higher Cr_2O_3 contents of PLZ garnet (Fig. 2).

Results of the melt-peridotite interaction experiments

The melt-peridotite interaction experiments were performed in order to investigate the reactivity of the melt compositions described in the earlier sections with depleted peridotitic material. For this purpose, dolomitic (Carmet) and silicate (Silmet) melt compositions, and two peridotitic protoliths were synthesized (Table 1). The interaction experiments were performed at 2.0 GPa and 1000 °C. Details of the experimental conditions and results are presented in Table 2. Reactions were obtained by least-squares mass-balance calculation of the proportion of the phases stable before and after each interaction.

Carmet-HAR interaction experiment

In addition to olivine and orthopyroxene present in the harzburgitic protolith, the product of the Carmet-HAR interaction experiment contains clinopyroxene and phlogopite (Table 2). Moreover, the absence of carbonates suggests the existence of a CO_2-rich low-density fluid. The metasomatic reaction between Carmet and HAR is (in weight proportion)

$$\begin{aligned} &24.8\ (\text{orthopyroxene})_{HAR} + 9.9\ \text{Carmet} \\ &\quad \rightarrow 14.2\ \text{olivine} + 13.6\ \text{clinopyroxene} \\ &\qquad + 2.7\ \text{phlogopite} + 4.2\ CO_2. \end{aligned} \tag{3}$$

This important transformation of the harzburgite by Carmet is related to the breakdown in peridotitic systems of dolomite at pressures less than 2.1 GPa (e.g., Wyllie and Rutter, 1986; Wallace and Green, 1988; Falloon and Green, 1989) according to the well-documented reaction:

$$\begin{aligned} &\text{dolomite} + \text{enstatite} \\ &\quad \rightarrow \text{diopside} + \text{forsterite} + CO_2 \end{aligned} \tag{4}$$

(e.g., Wyllie and Huang, 1976; Eggler, 1978; Brey et al., 1983). At 2.0 GPa, the decarbonation reaction (Reaction 4) occurs around 950 °C in carbonated and hydrated peridotite (e.g., Falloon and Green, 1989). Therefore, interaction of Carmet and harzburgite at temperatures less than 950 °C should probably result in the formation of dolomite and phlogopite without consumption of orthopyroxene (dolomite-bearing phlogopite harzburgite), rather than the products of Reaction 3.

Carmet-WHR interaction experiment

The resulting mineral assemblage of the Carmet-WHR interaction experiment (Table 2) contains a calcite solid solution ($CaCO_3 \approx 90$ mol%) and phlogopite, in addition to olivine, clinopyroxene, and spinel present in the wehrlitic protolith. The metasomatic reaction between Carmet and WHR is (in weight proportion)

$$\begin{aligned} &3.1\ (\text{clinopyroxene})_{WHR} + 0.3\ (\text{spinel})_{WHR} \\ &+ 9.8\ \text{Carmet} \\ &\quad \rightarrow 2.5\ \text{olivine} + 2.6\ \text{phlogopite} + 7.0\ \text{calcite} \\ &\qquad + 1.1\ CO_2. \end{aligned} \tag{5}$$

Silmet-HAR interaction experiment

The experimental conditions for the Silmet-HAR interaction (Table 2) were essentially the same as those for the Carmet-HAR experiment (2.0 GPa, 1000 °C), except that the starting mixture was first held at 1225 °C for 1 h to induce Silmet melting and then cooled slowly to 1000 °C (cf. Meen, 1987). The final product of the experiment using the Silmet composition and the harzburgite protolith consists of olivine, orthopyroxene, clinopyroxene, and phlogopite (Table 2). The reaction for this interaction is (in weight proportion)

$$3.3\ (\text{olivine})_{\text{HAR}} + 0.1\ (\text{orthopyroxene})_{\text{HAR}} + 10.0\ \text{Silmet} \rightarrow 7.2\ \text{clinopyroxene} + 6.2\ \text{phlogopite}. \quad (6)$$

In Reaction 6 most of the components required for the formation of the newly introduced clinopyroxene and phlogopite come from the crystallization of the silicate melt. Only the small excess of K_2O, Al_2O_3, SiO_2, and H_2O contained in Silmet, reflecting the incongruent melting of phlogopite to form olivine and liquid in the phlogopite lherzolite melting experiment, reacts with olivine of the harzburgite to form metasomatic phlogopite.

Implications of the interaction experiments

Figure 4a represents a summary of the mineralogical effects on a harzburgitic protolith, caused by the hypothetical infiltration of Carmet at 2.0 GPa and 1000 °C, depicted on an olivine-orthopyroxene-clinopyroxene ternary diagram. The harzburgite in Figure 4a contains 70 vol% of olivine and 30 vol% of orthopyroxene, a realistic average of the proportions found in many mantle xenoliths of harzburgitic compositions (e.g., Boyd, 1989). Approximately 12 g of Carmet would be needed to transform 100 g of harzburgite to an olivine-rich wehrlite (Fig. 4a) with about 3 vol% of phlogopite. Because of the high ratio of Mg/Fe of the dolomitic melt, the bulk $X_{\text{MgFe}_{\text{tot}}}$ of the wehrlite should be close to that of the protolith (cf. Green and Wallace, 1988). If Carmet infiltration persists, the metasomatized mantle would then evolve toward a calcite- and phlogopite-bearing dunite (Fig. 4a).

The mineralogical effects of Silmet infiltration in the harzburgite is transformation to an olivine-poor phlogopite lherzolite (Fig. 4a). Because Silmet reacts primarily with olivine in the Silmet-HAR interaction experiment, the same type of reaction (Reaction 6) should probably occur if Silmet infiltrated an olivine-rich wehrlite. The effect would then be to drive the composition toward an olivine-poor phlogopite wehrlite (Fig. 4a).

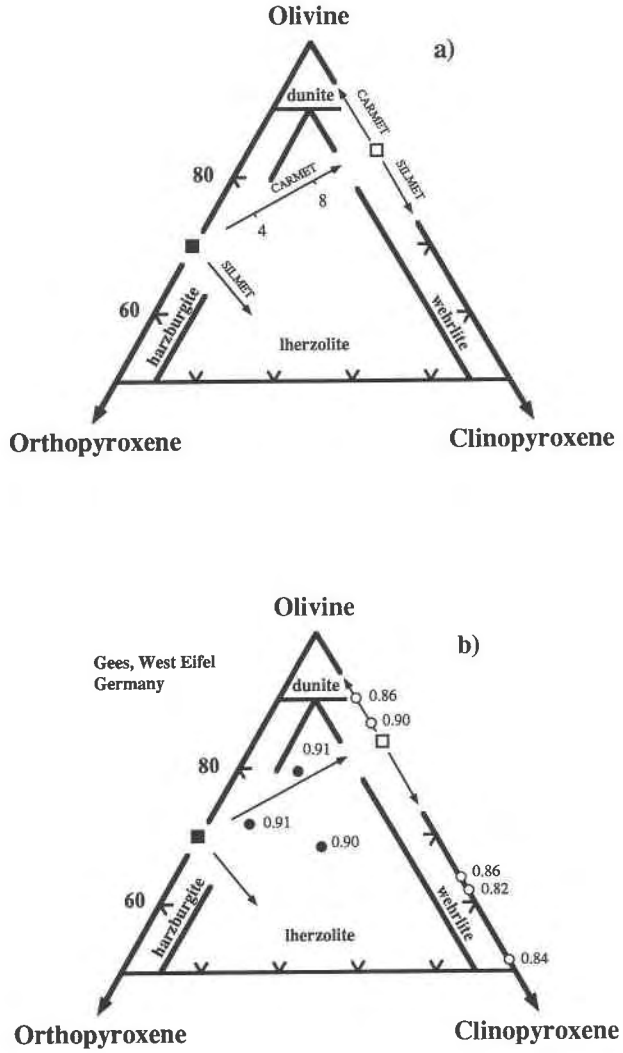

Fig. 4. **(a)** Effects of the progressive metasomatism (arrows) of a harzburgitic protolith at 2.0 GPa and 1000 °C caused by the infiltration of Carmet or Silmet. The trend from harzburgite (filled square) to olivine-rich wehrlite (empty square) caused by Carmet infiltration is graduated at intervals, indicating the amount of Carmet (in grams) needed for the transformation of 100 g of harzburgite protolith. More details in text. **(b)** Modal compositions of representative samples of the major types of peridotitic xenoliths collected from the mafic ashes in a quarry southeast of Gees, West Eifel, Germany, plotted in an olivine-orthopyroxene-clinopyroxene ternary diagram (cf. Fenwick, 1991). Each sample is labeled by a number representing the weighted average of the $X_{\text{MgFe}_{\text{tot}}}$ values calculated for all the silicate minerals. Filled circles are orthopyroxene-bearing xenoliths, and empty circles are orthopyroxene-free xenoliths. All data used for the construction of this diagram are taken from Edgar et al. (1989) and Lloyd et al. (1991). The metasomatic trends shown in **a** are superposed in **b**.

Petrological implications

In this section the experimental results are integrated into a petrological framework of cyclic metasomatic processes potentially active in the lithospheric mantle of a continental rift.

Multicycle metasomatic processes below a continental rift

A thermal framework. Figure 5 shows four geotherms representing the thermal evolution of the upper mantle

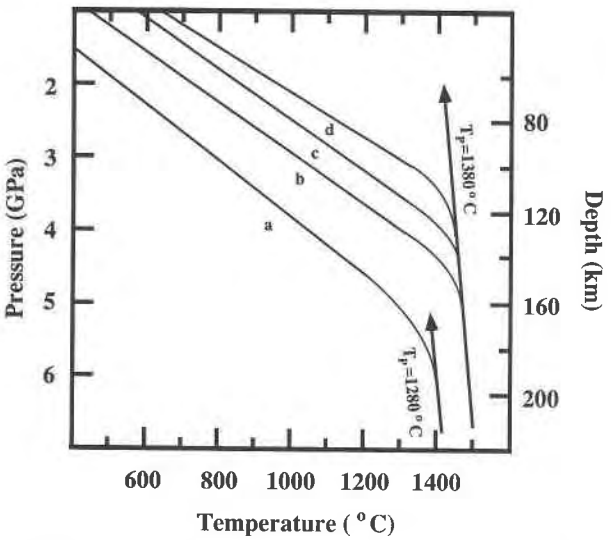

Fig. 5. Group of geotherms representing different hypothetical stages in the thermal evolution of the lithospheric mantle below a continental rift. Geotherm a is considered characteristic of the lithospheric mantle before initiation of rifting and is taken from McKenzie (1989, his Fig. 4d). Geotherms b, c, and d depict the thermal disturbances during progressive rifting related to the adiabatic ascent of a hot mantle plume with a potential temperature (T_p) of 1380 °C. Geotherms b and c are not derived from any data or calculations but are considered reasonable intermediates between geotherms a and d. The temperatures defined by geotherm d up to 3.0 GPa are comparable to the ones proposed by Seck and Wedepohl (1983) and Fuchs and Wedepohl (1983) for the Rhenish Massif, Germany. The potential temperature is the temperature that the mantle would have if it could rise to the Earth's surface under perfect adiabatic conditions (e.g., McKenzie and Bickle, 1988).

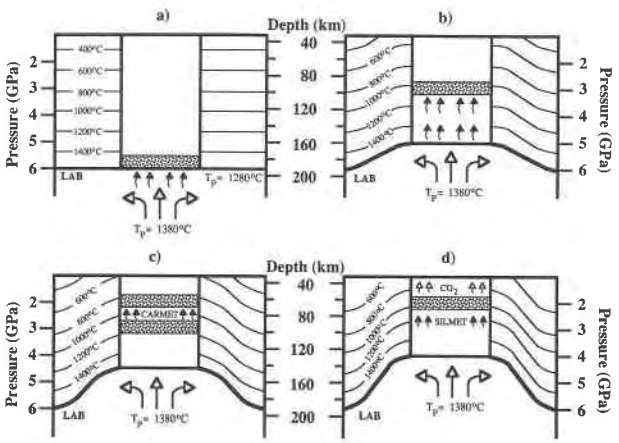

Fig. 6. Hypothetical schematic sections representing the thermal conditions in the lithospheric mantle below a continental rift. The sketches at the center of each section illustrate the proposed metasomatic processes in a portion of the lithospheric mantle originally harzburgitic in composition. The intersections of the isotherms with the central sketches define the pressure-temperature conditions corresponding to the geotherms of Figure 5: (**a**) geotherm a, (**b**) geotherm b, (**c**) geotherm c, and (**d**) geotherm d. The curvatures of the isotherms are purely qualitative but emphasize the thermal disturbances accompanying lithospheric thinning relative to the original thermal conditions shown in **a.** LAB refers to the lithosphere-asthenosphere boundary. The patterned areas represent the metasomatic horizons. Large empty arrows = adiabatic upwelling of hot mantle plume (T_p 1380 °C); small filled arrows = infiltration of small fractions of melts or dense fluids; small empty arrows = release of CO_2-rich low-density fluid; Carmet = alkaline dolomitic melt; Silmet = hydrous potassic and calcic silicate melt. More details in text.

below a hypothetical active continental rift. The progressive thinning of the lithosphere and the associated thermal disturbances are depicted as the result of the adiabatic upwelling of a mantle plume with a potential temperature of 1380 °C. Simplified schematic sections depicting the proposed processes occurring in a lithospheric mantle of harzburgitic composition are shown in Figure 6.

Deep metasomatic cycles (depth >100 km). In Figure 6a, the fertile mantle plume releases fluids as it reaches the lithosphere-asthenosphere boundary (LAB) (e.g., Wyllie, 1988, his Figs. 45 and 46). Diamond microinclusions whose compositions resemble that of potassic magmas but with volatile contents (essentially H_2O and CO_2) up to 40% may represent such high-pressure (>5.0 GPa) fluids (Navon et al., 1988). Because these volatile-rich inclusions are rich in K_2O, CaO, SiO_2, and FeO (Navon et al., 1988, their Table 1), they should be effective in transforming harzburgite into carbonated phlogopite lherzolite.

As the LAB progressively rises (Fig. 6b), the carbonated phlogopite lherzolite partially melts because of heat conduction from the underlying plume and decompression caused by uplift (e.g., McKenzie, 1989). The low-temperature melting components are then remobilized in small-volume volatile-rich melts, which, as they migrate upward, resolidify and react with the overlying colder harzburgite. Through such cycles of melting, migrating, solidifying, and reacting, the metasomatic front eventually reaches a depth of 100 km (≈3.0 GPa). The temperature at that depth being approximately 1050 °C (Fig. 6b), the interaction of the CO_2- and H_2O-bearing melts with harzburgite results in the formation of a dolomite-bearing phlogopite lherzolite.

Shallow decoupled metasomatic cycle (depth <100 km). In Figure 6c, the temperature of the horizon of dolomite-bearing phlogopite lherzolite at a depth of 100 km is raised to about 1150 °C. An alkaline dolomitic melt can form and infiltrate the overlying depleted lithosphere, leaving residual CO_2-free garnet-bearing phlogopite lherzolite, which returns to subsolidus conditions (e.g., PLZ, Table 2). As the alkaline dolomitic melt reaches a depth of about 65 km (≈2.0 GPa, <950 °C), it solidifies and reacts with harzburgite, resulting in the formation of a dolomite-bearing phlogopite harzburgite. The metasomatic front is now decoupled and forms two distinct horizons: a dolomite-bearing phlogopite harzburgite at 65 km and a CO_2-free garnet-bearing phlogopite lherzolite at 100 km.

With progressive rifting, the temperature at a depth of

65 km reaches 1000 °C (Fig. 6d). The dolomite-bearing phlogopite harzburgite is then transformed to olivine-rich phlogopite lherzolite and wehrlite, with the release of CO_2-rich low-density fluid (see Reaction 3). At 100 km, the temperature of the garnet-bearing phlogopite lherzolite horizon exceeds the solidus, forming a hydrous potassic and calcic silicate melt. When this melt infiltrates the metasome at the depth of 65 km, an enrichment in clinopyroxene and phlogopite takes place, according to Reaction 6. Because the silicate melt has a lower Mg/Fe ratio, a decrease in the bulk $X_{MgFe_{tot}}$ is also expected. The final product of this shallow decoupled metasomatic cycle is a wide variety of rock types comparable to those depicted in Figure 4a.

The Eifel mantle xenoliths—an example of a shallow decoupled metasomatic event?

Recently, Edgar et al. (1989) and Lloyd et al. (1991) studied a group of 225 ultramafic xenoliths sampled from mafic ashes near Gees village, in the West Eifel sodipotassic volcanic region, Germany. The majority of the xenoliths (≈87%) are peridotitic, ranging from spinel harzburgite and spinel lherzolite to olivine-rich and olivine-poor spinel wehrlite, with various amounts of phlogopite (Lloyd et al., 1991). In wehrlite, as the amount of olivine decreases, the abundance of titaniferous phlogopite increases. In Figure 4b, peridotitic samples studied by Edgar et al. (1989) and Lloyd et al. (1991) are plotted on an olivine-orthopyroxene-clinopyroxene ternary diagram.

It is suggested that the proposed decoupled metasomatic process is compatible with the compositional variation observed in the Gees xenoliths. The major points supporting this suggestion are

1. The compositional variations of the xenoliths are consistent with the trends that the decoupled metasomatic process may create (Fig. 4b) at thermal conditions of geotherm d (Fig. 5) and pressures near or less than 2.0 GPa. These conditions are probably characteristic of the mantle represented by the Gees xenoliths because (a) geotherm d is based on data from the Rhenish Massif, and (b) the peridotite xenoliths contain chromium spinel and are garnet free, suggesting pressures less than 2.5 GPa (e.g., Carroll Webb and Wood, 1986).

2. The common source of the metasomatic agents is a carbonated phlogopite lherzolite horizon near the depth of 100 km. Such a horizon at this depth was proposed by Mertes and Schmincke (1985) as the source for some of the potassic lavas erupted in the West Eifel area.

3. Except for one sample, all the olivine-rich rocks (>65 vol% olivine) following the trend from harzburgite to olivine-rich wehrlite have constant average silicate $X_{MgFe_{tot}}$ values of 0.90 and 0.91 (Fig. 4b), compatible with the metasomatic effects of a primitive carbonatite melt. All the olivine-poor xenoliths have significantly lower $X_{MgFe_{tot}}$ (≤0.86, Fig. 4b), in accordance with a silicate melt infiltration event. The olivine-rich rock with an $X_{MgFe_{tot}}$ value of 0.86 is, in contrast to the others, very rich in phlogopite (≈11 vol%; Lloyd et al., 1991), and therefore may have been infiltrated by a K-rich derivative of the alkali-rich silicate melt.

Acknowledgments

Financial support was provided by a NSERC grant to A.D.E. and a FCAR scholarship to Y.T. Funding from NATO as a Collaborative Research Grant is acknowledged. Danilo Vukadinovic and Sandro Conticelli are thanked for helpful discussions. Constructive reviews by David H. Green, David Hay, and Richard F. Wendlandt are appreciated.

References cited

Ballhaus, C., Berry, R.F., and Green, D.H. (1991) High pressure experimental calibration of the olivine-orthopyroxene-spinel oxygen geobarometer: Implications for the oxidation state of the upper mantle. Contributions to Mineralogy and Petrology, 107, 27–40.

Boyd, F.R. (1989) Compositional distinction between oceanic and cratonic lithosphere. Earth and Planetary Science Letters, 96, 15–26.

Boyd, F.R., and England, J.L. (1960) Apparatus for phase equilibrium measurements at pressures up to 50 kbar and temperatures to 1750 °C. Journal of Geophysical Research, 65, 741–748.

Brey, G., Brice, W.R., Ellis, D.J., Green, D.H., Harris, K.L., and Ryabchikov, I.D. (1983) Pyroxene-carbonate reactions in the upper mantle. Earth and Planetary Science Letters, 62, 63–74.

Canil, D. (1990) Experimental study bearing on the absence of carbonate in mantle-derived xenoliths. Geology, 18, 1011–1013.

Carroll Webb, S.A., and Wood, B.J. (1986) Spinel-pyroxene-garnet relationships and their dependence on Cr/Al ratio. Contributions to Mineralogy and Petrology, 92, 471–480.

Edgar, A.D., Lloyd, F.E., Forsyth, D.M., and Barnett, R.L. (1989) Origin of glass in upper mantle xenoliths from the quaternary volcanics of Gees, West Eifel, Germany. Contributions to Mineralogy and Petrology, 103, 277–286.

Eggler, D.H. (1978) The effect of CO_2 upon partial melting of peridotite in the system Na_2O-CaO-Al_2O_3-MgO-SiO_2-CO_2 to 35 kb, with an analysis of melting in a peridotite-H_2O-CO_2 system. American Journal of Science, 278, 305–343.

Erlank, A.J., Waters, F.G., Hawkesworth, C.J., Haggerty, S.E., Allsopp, H.L., Rickard, R.S., and Menzies, M.A. (1987) Evidence of mantle metasomatism in peridotite nodules from the Kimberley pipes, South Africa. In M.A. Menzies and C.J. Hawkesworth, Eds., Mantle metasomatism, p. 221–311. Academic Press, London.

Falloon, T.J., and Green, D.H. (1989) The solidus of carbonated fertile peridotite. Earth and Planetary Science Letters, 94, 364–370.

Fenwick, C.S. (1991) Petrographic and geochemical heterogeneity in mantle xenoliths from the Quaternary lavas of the West Eifel: Implications for mantle metasomatism beneath the Rhenish Massif, 187 p. Ph.D. thesis, University of Reading, Reading, U.K.

Fuchs, K., and Wedepohl, K.H. (1983) Relation of geophysical and petrological models of upper mantle structure of the Rhenish Massif. In K. Fuchs, K. von Gehlen, H. Mälzer, H. Murawski, and A. Semmel, Eds., Plateau uplift—The Rhenish shield—A case history, p. 352–363. Springer Verlag, Berlin.

Fujii, T., and Scarfe, C.M. (1985) Composition of liquids coexisting with spinel lherzolite at 10 kbar and the genesis of MORBs. Contributions to Mineralogy and Petrology, 90, 18–28.

Green, D.H., and Ringwood, A.E. (1970) Mineralogy of peridotitic compositions under upper mantle conditions. Physics of the Earth and Planetary Interiors, 3, 359–371.

Green, D.H., and Wallace, M.E. (1988) Mantle metasomatism by ephemeral carbonatite melts. Nature, 336, 459–462.

Harte, B., and Hawkesworth, C.J. (1989) Mantle domains and mantle xenoliths. In J. Ross, A.L. Jaques, J. Ferguson, D.H. Green, S.Y. O'Reilly, R.V. Danchin, and A.S.A. Janse, Eds., Kimberlites and related rocks: Their mantle/crust setting, diamonds and diamond exploration. Geological Society of Australia, Special Publication 14, vol. 2, p. 649–686. Blackwell, Victoria, British Columbia, Canada.

Holloway, J.R., and Eggler, D.H. (1976) Fluid-absent melting of peridotite containing phlogopite and dolomite. Carnegie Institution of Washington Year Book, 75, 636–639.

Hunter, R.H., and McKenzie, D. (1989) The equilibrium geometry of carbonate melts in rocks of mantle composition. Earth and Planetary Science Letters, 92, 347–356.

Kress, V.C., and Carmichael, I.S.E. (1988) Stoichiometry of the iron oxidation reaction in silicate melts. American Mineralogist, 73, 1267–1274.

Lloyd, F.E., Edgar, A.D., Forsyth, D.M., and Barnett, R.L. (1991) The paragenesis of upper mantle xenoliths from the Quaternary volcanics south-east of Gees, West Eifel, Germany. Mineralogical Magazine, 55, 95–112.

Mattioli, G.S., Baker, M.B., Rutter, M.J., and Stolper, E.M. (1989) Upper mantle oxygen fugacity and its relationship to metasomatism. Journal of Geology, 97, 521–536.

McKenzie, D. (1985) The extraction of magma from the crust and mantle. Earth and Planetary Science Letters, 74, 81–91.

——— (1989) Some remarks on the movement of small melt fractions in the mantle. Earth and Planetary Science Letters, 95, 53–72.

McKenzie, D., and Bickle, M.J. (1988) The volume and composition of melt generated by extension of the lithosphere. Journal of Petrology, 29, 625–679.

Meen, J.K. (1987) Mantle metasomatism and carbonatites; an experimental study of a complex relationship. Geological Society of America, Special Paper 215, 91–100.

Meen, J.K., Ayers, J.C., and Fregeau, E.J. (1989) A model of mantle metasomatism by carbonated alkaline melts: Trace-element and isotopic compositions of mantle source regions of carbonatite and other continental igneous rocks. In K. Bell, Ed., Carbonatites—Genesis and evolution, p. 464–499. Unwin Hyman, London.

Mengel, K., and Green, D.H. (1989) Stability of amphibole and phlogopite in metasomatized peridotite under water-saturated and water-undersaturated conditions. In J. Ross, A.L. Jaques, J. Ferguson, D.H. Green, S.Y. O'Reilly, R.V. Danchin, and A.S.A. Janse, Eds., Kimberlites and related rocks: Their composition, occurrence, origin and emplacement. Geological Society of Australia, Special Publication 14, vol. 1, p. 571–581. Blackwell, Victoria, British Columbia, Canada.

Mertes, H., and Schmincke, H.-U. (1985) Mafic potassic lavas of the Quaternary West Eifel volcanic field. Contributions to Mineralogy and Petrology, 89, 330–345.

Myers, J., and Eugster, H.P. (1983) The system Fe-Si-O: Oxygen buffer calibrations to 1500 K. Contributions to Mineralogy and Petrology, 82, 75–90.

Navon, O., Hutcheon, I.D., Rossman, G.R., and Wasserburg, G.J. (1988) Mantle-derived fluids in diamond micro-inclusions. Nature, 335, 784–789.

Olafsson, M., and Eggler, D.H. (1983) Phase relations of amphibole, amphibole-carbonate, and phlogopite-carbonate peridotite: Petrologic constraints on the asthenosphere. Earth and Planetary Science Letters, 64, 305–315.

Seck, H.A., and Wedepohl, K.H. (1983) Mantle xenoliths in the Rhenish Massif and the northern Hessian Depression. In K. Fuchs, K. von Gehlen, H. Mälzer, H. Murawski, and A. Semmel, Eds., Plateau uplift—The Rhenish shield—A case history, p. 343–351. Springer-Verlag, Berlin.

Spera, F.J. (1984) Carbon dioxide in petrogenesis III: Role of volatiles in the ascent of alkaline magma with special reference to xenolith-bearing mafic lavas. Contributions to Mineralogy and Petrology, 88, 217–232.

Wallace, M.E., and Green, D.H. (1988) An experimental determination of primary carbonatite magma composition. Nature, 335, 343–346.

Wendlandt, R.F., and Eggler, D.H. (1980) The origins of potassic magmas: 2. Stability of phlogopite in natural spinel lherzolite and in the system $KAlSiO_4$-MgO-SiO_2-H_2O-CO_2 at high pressures and high temperatures. American Journal of Science, 280, 421–458.

Wyllie, P.J. (1988) Magma genesis, plate tectonics, and chemical differentiation of the earth. Reviews of Geophysics, 26, 370–404.

Wyllie, P.J., and Huang, W.-L. (1976) Carbonation and melting reactions in the system CaO-MgO-SiO_2-CO_2 at mantle pressures with geophysical and petrological applications. Contributions to Mineralogy and Petrology, 54, 79–107.

Wyllie, P.J., and Rutter, M. (1986) Experimental data on the solidus for peridotite-CO_2, with applications to alkaline magmatism and mantle metasomatism. Eos, 67, 390.

Manuscript received September 6, 1991
Manuscript accepted March 13, 1992